The Stereodynamics of 1,2-Dipropyldiaziridines

OLIVER TRAPP,[1,2]* LAILA SAHRAOUI,[2] WERNER HOFSTADT,[2] AND WERNER KÖNEN[2]
[1]*Organisch-Chemisches Institut, Ruprecht-Karls-Universität Heidelberg, Heidelberg, Germany*
[2]*Max-Planck-Institut für Kohlenforschung, Mülheim an der Ruhr, Germany*

ABSTRACT N-alkylated *trans*-diaziridines are an intriguing class of compounds with two stereogenic nitrogen atoms which easily interconvert. In the course of our investigations of the nature of the interconversion process via nitrogen inversion or electrocyclic ring opening ring closure, we synthesized and characterized the three constitutionally isomeric diaziridines 1,2-di-*n*-propyldiaziridine **1**, 1-isopropyl-2-*n*-propyldiaziridine **2**, and 1,2-diisopropyldiaziridine **3** to study the influence of the substituents on the interconversion barriers. Enantiomer separation was achieved by enantioselective gas chromatography on the chiral stationary phase Chirasil-β-Dex with high separation factors α (1-isopropyl-2-*n*-propyldiaziridine: 1.18; 1, 2-diisopropyldiaziridine: 1.24; 100°C 50 kPa He) for the isopropyl substituted diaziridines. These compounds showed pronounced plateau formation between 100 and 150°C, and peak coalescence at elevated temperatures. The enantiomerization barriers $\Delta G^{\ddagger}$ and activation parameters $\Delta H^{\ddagger}$ and $\Delta S^{\ddagger}$ were determined by enantioselective dynamic gas chromatography (DGC) and direct evaluation of the elution profiles using the unified equation implemented in the software DCXplorer. Interestingly, 1-isopropyl-2-*n*-propyldiaziridine and 1,2-diisopropyldiaziridine exhibit similar high interconversion barriers $\Delta G^{\ddagger}$ (100°C) of 128.3 ± 0.4 kJ mol^{-1} and 129.8 ± 0.4 kJ mol^{-1}, respectively, which indicates that two sterically demanding substituents do not substantially increase the barrier as expected for a distinct nitrogen inversion process. *Chirality 22:284–291, 2010.*

KEY WORDS: activation barrier; chiral separation; stereogenic nitrogen; enantioselective dynamic gas chromatography; interconversion; kinetics; unified equation

INTRODUCTION

The investigation of conformational and configurational changes,[1,2] e.g., isomerizations, epimerizations, diastereomerizations, and enantiomerizations,[3] is of great importance to understand processes ranging from protein folding to the stereostability of drugs. Compounds with stereogenic nitrogen atoms are an intriguing class of compounds that have inspired many scientists for more than a century. In 1890, Werner[4] transferred the concept of tetrahedral tetravalent carbon of van't Hoff and Le Bel to trivalent nitrogen. Attempts made by Meisenheimer et al. to isolate chiral tertiary amines of the type *NRR′R″* suggested that rapid pyramidal inversion leads to optical inactivity.[5] In 1944, Prelog and Wieland[6] recognized the inherent chirality of Tröger's base[7] due to the two stereogenic nitrogen atoms related by C2 symmetry. They achieved enantiomer separation by liquid chromatography on a 0.9 m column using lactose hydrate as CSP (op = 0.99), followed by fractional crystallization. In 1967, Mannschreck et al.[8] reported that nitrogen inversion in diaziridines (cf. Scheme 1) is hindered on the NMR time scale and determined later interconversion barriers by dynamic NMR (DNMR).[9,10]

To achieve the isolation of stereoisomers with stereogenic nitrogen, two strategies have been successfully applied by Brois,[11] Felix and Eschenmoser,[12] Lehn and Wagner,[13] and Kostyanovsky et al.[14] in 1968: (i) Introduction of lone-pair containing substituents (-OR, Cl, F) at the stereogenic nitrogen atom,[15,16] and (ii) incorporation of stereogenic nitrogen into a constrained (three-membered) ring.[17] This was demonstrated by the enantiomer separation of 1-chloroaziridines,[11–13,18] 1-alkoxyoxazolidines[19] and by the enantiomeric or diastereomeric enrichment of dialkoxyamines, containing the asymmetric nitrogen solely in the open chain. Despite these efforts, the nature of the interconversion process in aziridines and diaziridines via nitrogen inversion[20–23] as in ammonia, or electrocyclic ring opening ring closure as in oxiranes[24–26] is still unknown (cf. Scheme 1). Highly negative activation entropies $\Delta S^{\ddagger}$ were experimentally measured for aziridines and diaziridines, which were interpreted as an indicator of an

Contract grant sponsor: Deutsche Forschungsgemeinschaft for an Emmy Noether grant; Contract grant number: TR 542/3.
Contract grant sponsors: Max-Planck-Institut für Kohlenforschung, Fond der Chemischen Industrie (FCI), Merck Research Laboratories (Rahway, NJ), Nordrhein-Westfälische Akademie der Wissenschaften.
*Correspondence to: Oliver Trapp, Organisch-Chemisches Institut, Ruprecht-Karls-Universität Heidelberg, Im Neuenheimer Feld 270, 69120 Heidelberg, Germany. E-mail: trapp@oci.uni-heidelberg.de
Received for publication 10 June 2008; Accepted 25 March 2009
DOI: 10.1002/chir.20742
Published online 3 June 2009 in Wiley InterScience (www.interscience.wiley.com).

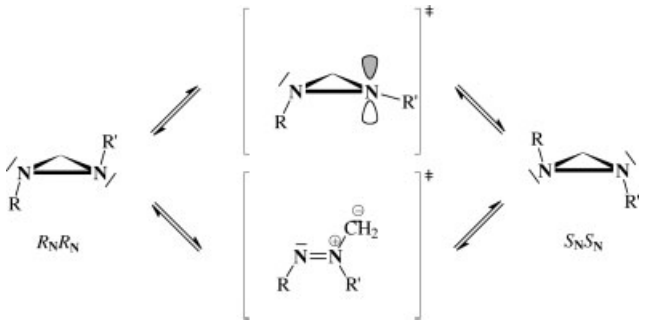

Scheme 1. Enantiomerization of *trans*-1,2-disubstituted diaziridines and possible mechanism of interconversion via nitrogen inversion (top) or electrocyclic ring opening ring closure mechanism.

electrocyclic ring opening-ring closure mechanism because of the charge separation in the transition state. In an effort to elucidate the mechanism of interconversion, we synthesized the set of the three constitutionally isomeric of *N*-propyl substituted diaziridines 1,2-di-*n*-propyldiaziridine **1**, 1-isopropyl-2-*n*-propyldiaziridine **2**, and 1,2-diisopropyldiaziridine **3** (cf. Scheme 2). 3,3-Unsubstituted diaziridines are of great interest because the barrier is increased due to the lack of 1,2-nonbonded interactions which destabilize the ground state.[27]

These diaziridines were chosen, because increasing the steric demand by introduction of a methyl group at the α-C atom of the substituent is more effective for shorter than for longer alkyl groups without introducing further stereogenic centers, e.g., for *sec*-butyl substituents. Furthermore, it is expected that if the interconversion barrier depends on the steric hindrance of the substitutents in a distinct inversion process, the barrier of the heterosubstituted diaziridine **2** should be the average of the barriers of the homosubstituted diaziridines **1** and **2**.

To study conformational and configurational changes in molecules, sophisticated techniques were developed which require only racemic mixtures to quantify interconversion kinetics, e.g., dynamic NMR,[28,29] stopped-flow chromatographic techniques,[30–33] and enantioselective dynamic chromatography.[34–38] Enantioselective dynamic chromatography has been used for the determination of the kinetics of stereolabile compounds, e.g., atropisomers, drugs and drug-related compounds, compounds with stereogenic nitrogen and sulfur, and pheromones covering the range of interconversion barriers $\Delta G^{\ddagger}$ between 75 and 170 kJ mol^{-1}. Depending on the physical properties of the analyte molecule and the expected interconversion barrier, different dynamic chromatographic or electrophoretic techniques (e.g., DGC, DSFC, DHPLC, DCE, DCEC, DMEKC) can be applied to determine interconversion barriers. The major advantage over classical racemization experiments, which require enantiomer separation of stereolabile compounds, are the use of standard experimental setups, the minute analyte consumption of arbitrary mixtures of interconverting stereoisomers and the precise determination of kinetic and thermodynamic parameters.

In enantioselective dynamic chromatography, peak profiles are characterized by peak broadening, plateau formation, and eventually peak coalescence.[39] The pronounced plateau formation and separation of the stereoisomers are the prerequisite for the determination of interconversion barriers in dynamic chromatography.

In recent years, considerable progress has been made to determine reaction rate constants *k* and activation parameters from elution profiles of dynamic chromatographic experiments. Broadly used are computer simulations based on the iterative comparison of experimental and simulated chromatograms,[40–42] which are computationally expensive for highly efficient separation techniques with theoretical plate numbers *N* greater than 20,000. In 2001, the approximation function[43,44] was introduced for fast, direct, and precise access to rate constants to study enantiomerization of racemic mixtures. A major breakthrough was the derivation of the unified equation[45–47] to access directly all kinds of first-order reactions taking place during a chromatographic or electrophoretic separation. This equation is an analytical solution of the theoretical plate model and is superior in precision to any computer simulation where errors arise from the imprecision of billions of floating point operations. The unified equation also opened the field to study catalytic reactions by on-column reaction chromatography[48–52] in a high-throughput fashion.[53]

MATERIALS AND METHODS

General

n-Propylamine, isopropylamine, formaldehyde, sodium hydroxide, and sodium hypochlorite were purchased from Fluka (Buchs, Switzerland). Nuclear magnetic resonance (^{1}H-NMR and ^{13}C-NMR) spectra were recorded at 400 and 100 MHz, respectively, on a Bruker AV 400 spectrometer (Rheinstetten, Germany) in deuterochloroform. Electron impact mass spectra (EIMS, ion source temperature 200°C, electron energy 70 eV) were recorded on a Thermo GC quadrupole-ion trap mass spectrometer Trace GC PolarisQ (San Jose, CA).

General Procedure for the Synthesis of 1,2-Substituted Diaziridines 1, 2, and 3

The diaziridines were prepared according to a modification of the method Ohme et al.[47,54] 250 mmol Alkylamine and 50 ml 5N NaOH are combined in a 250 ml flask

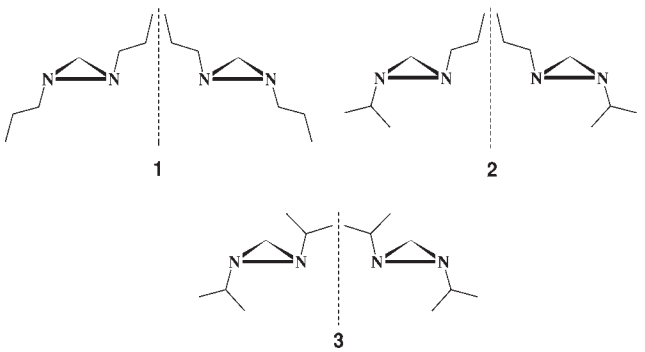

Scheme 2. Enantiomeric pairs of (a) 1,2-di-*n*-propyldiazirine 1, (b) 1-isopropyl-2-*n*-propyldiaziridine 2, and (c) 1,2-diisopropyldiaziridine 3.

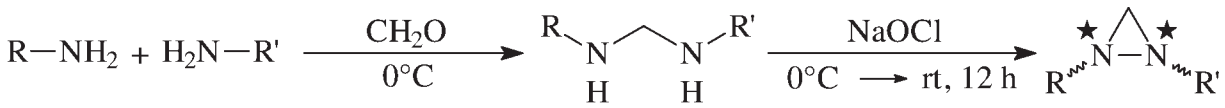

Scheme 3. Statistical synthesis of 1,2-homosubstituted and 1,2-heterosubstituted diaziridines by formation of the aminal from amines using formaldehyde, followed by an oxidative ring closure with sodium hypochlorite solution.

equipped with a magnetic stirrer and cooled to 0°C. Formaldehyde solution (36% w/w, 12.5 ml) is slowly added. After 1 h, 75 ml sodium hypochlorite solution (13% w/w) is added dropwise at 0°C and after complete addition the mixture is allowed to warm up to r.t. The mixture is stirred at r.t. for 12 h, then after 1 h waiting for phase separation the organic layer is separated and washed with diluted sodium thiosulfate solution and water. After drying over KOH and filtration the crude diaziridine is distilled under reduced pressure.

1,2-Di-*n*-propyldiaziridine. 1,2-Di-*n*-propyldiaziridine **1** is obtained as a colorless liquid in 22.5% (3.6 g) yield. bp 37°C (37 mbar); ^{1}H-NMR ($CDCl_3$) δ 0.95 (t, $^3J(H,H)$ = 7.4 Hz, 6H, CH^3), 1.61 (m, $^3J(H,H)$ = 7.4 Hz, 4H, CH_2), 2.21 (m, $^3J(H,H)$ = 7 Hz, $2H^a$, CH_2—N), 2.42 (m, $^3J(H,H)$ = 7 Hz, $2H^b$, CH_2—N), 2.44 (s, 2H, N—CH_2—N); ^{13}C-NMR ($CDCl_3$) δ 11.5 (CH_3), 21.6 (CH_2), 56.4 (N—CH_2—N), 62.8 (CH_2—N); MS *m/z* (relative intensity) 128.07 (M^+, 0.63), 100.14 (2.85), 99.1 (47), 86.13 (1.6), 85.12 (8.42), 72.11 (7.12), 71.07 (28.12), 70.08 (8.08), 68.13 (1.3), 58.09 (7.32), 57.04 (100), 56.09 (6.3), 55.14 (0.72), 54.1 (1.75), 51.98 (1.36).

1-Isopropyl-2-*n*-propyldiaziridine. 1-Isopropyl-2-*n*-propyldiaziridine **2** is obtained as a colorless liquid in 16.4% (2.66 g) yield. bp 44°C (67 mbar); ^{1}H-NMR ($CDCl_3$) δ 0.95 (t, $^3J(H,H)$ = 7.4 Hz, 3H, CH_3, *n*-propyl), 1.04 (d, $^3J(H,H)$ = 6.4 Hz, $3H^a$, CH_3, isopropyl), 1.2 (d, $^3J(H,H)$ = 6.4 Hz, $3H^b$, CH_3, isopropyl), 1.62 (m, $^3J(H,H)$ = 7.4 Hz, 2H, CH_2, *n*-propyl), 1.72 (m, $^3J(H,H)$ = 6.4 Hz, 1H,

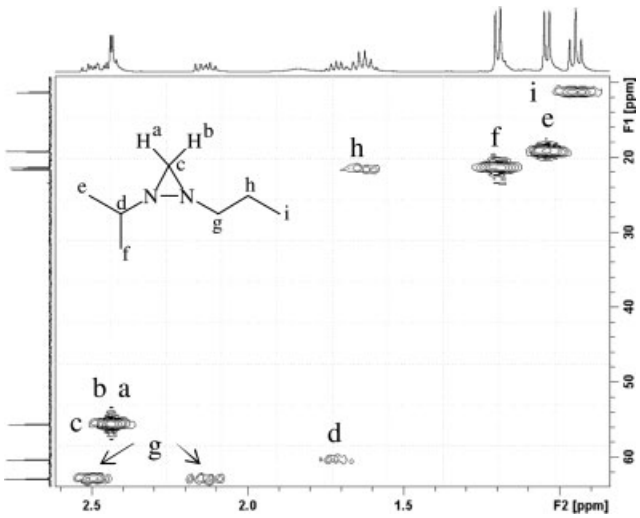

Fig. 1. ^{1}H-^{13}C correlation NMR spectrum of 1-isopropyl-2-*n*-propyldiaziridine **2**.

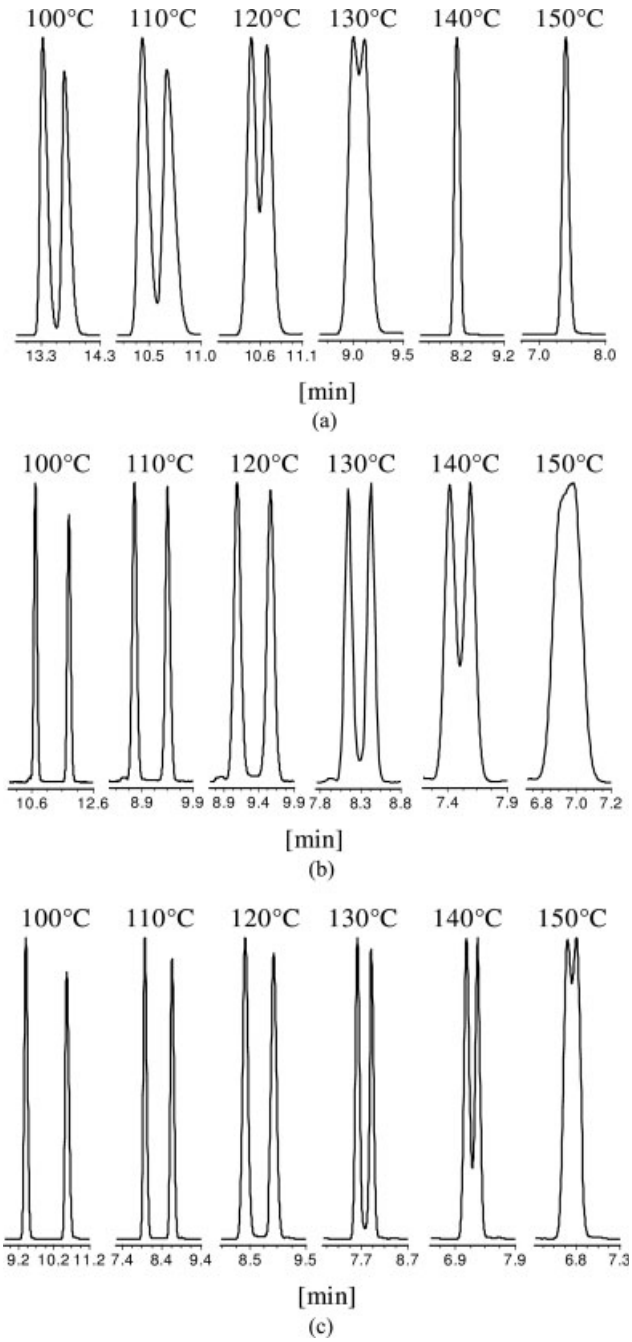

Fig. 2. Selected experimental enantiomerization profiles of the enantioselective DGC experiments. (**a**) 1,2-Di-*n*-propyldiazirine **1**, (**b**) 1-isopropyl-2-*n*-propyldiaziridine **2**, and (**c**) 1,2-diisopropyldiaziridine **3** separated between 100 and 150°C. Chromatographic conditions: 25 m Chirasil-β-Dex (0.25 mm i.d., film thickness 0.5 μm). Carrier gas: He.

TABLE 1. Experimental data of the enantiomerization of 1,2-diisopropyldiaziridine 3 between 100 and 140°C

T (°C)	p (kPa)	t_R^A (min)	t_R^B (min)	N	α	h_p (%)	h_B (%)	k_1 (10^{-4} s^{-1})
100.0	50.0	9.4	10.5	40,100	1.24	0.1	88.6	0.05
100.0	50.0	9.4	10.5	41,900	1.24	0.1	87.0	0.06
100.0	50.0	9.4	10.5	42,800	1.24	0.1	89.1	0.05
110.0	50.0	7.9	8.6	35,200	1.22	0.2	92.4	0.13
110.0	50.0	7.9	8.6	33,400	1.21	0.2	92.9	0.14
110.0	50.0	7.9	8.6	41,700	1.22	0.2	93.0	0.15
120.0	40.0	8.4	8.9	31,800	1.18	0.7	95.5	0.32
120.0	40.0	8.4	8.9	32,400	1.18	0.8	94.9	0.37
120.0	40.0	8.4	8.9	34,000	1.18	0.7	94.3	0.32
130.0	40.0	7.6	7.9	30,200	1.15	3.5	96.3	0.94
130.0	40.0	7.6	7.9	28,100	1.15	3.6	97.0	0.95
130.0	40.0	7.7	7.9	30,100	1.15	3.5	95.4	0.94
140.0	40.0	7.1	7.3	29,500	1.12	23.8	98.3	1.98
140.0	40.0	7.1	7.3	27,200	1.12	23.5	98.8	1.23
140.0	40.0	7.1	7.3	27,200	1.12	23.3	95.7	1.30

Chromatographic conditions: 25 m Chirasil-β-Dex (0.25 mm i.d.; film thickness 0.5 μm). Carrier gas: He.

CH—N), 2.13 (m, $^3J(H,H)$ = 7.4 Hz, 1H, CH_2—N), 2.44 (d, $^2J(H,H)$ = 2.7 Hz, 2H, N—CH_2—N), 2.49 (m, $^3J(H,H)$ = 7.4 Hz, 1H, CH_2—N); ^{13}C-NMR ($CDCl_3$) δ 11.4 (CH_3, *n*-propyl), 19.3 (C^aH_3, isopropyl), 21.4 (C^bH_3, isopropyl), 21.7 (CH_2), 55.7 (N—CH_2—N), 60.4 (CH—N), 63.0 (CH_2-N); MS *m/z* (relative intensity) 128.1 (M^+, 0.79), 113.13 (27.84), 99.12 (24.02), 86.13 (3.2), 85.09 (30.5), 72.12 (8.34), 71.09 (43.95), 70.12 (6.64), 59.1 (2.21), 58.08 (18.7), 57.06 (100), 56.08 (30.64), 55.12 (2.2), 54.11 (3.25), 51.98 (2.15).

1,2-Diisopropyldiaziridine. 1,2-Diisopropyldiaziridine **3** is obtained as a colorless liquid in 38.5% (6.2 g) yield. bp 26°C (61 mbar); ^{1}H-NMR ($CDCl_3$) δ 1.71 (d, $^3J(H,H)$ = 6.4 Hz, $6H^a$, CH_3), 1.21 (d, $^3J(H,H)$ = 6.4 Hz, $6H^b$, CH_3), 1.71 (m, $^3J(H,H)$ = 6.4 Hz, 2H, CH), 2.42 (s, 2H, N—CH_2—N); ^{13}C-NMR ($CDCl_3$) δ 19.3 (C^aH_3), 21.5 (C^bH_3), 54.8 (N—CH_2—N), 60.4 (CH); MS *m/z* (relative intensity) 128.07 (M^+, 1.39), 114.14 (4.69), 113.1 (61.44), 86.08 (1.06), 85.14 (1.75), 82.14 (2.14), 72.12 (5.64), 71.07 (100), 70.14 (2.75), 69.14 (1.36), 58.11 (11.54), 57.12 (2.07), 56.08 (32.15), 55.11 (1.21), 54.1 (2.55).

Enantioselective Dynamic Gas Chromatography

Dynamic gas chromatography was performed on a Thermo Trace PolarisQ GC-MS equipped with a split injector (250°C) and a flame-ionisation detector (250°C). For the separation of the enantiomers of 1,2-di-*n*-propyldiazirine **1**, 1-isopropyl-2-*n*-propyldiaziridine **2**, and 1,2-diisopropyldiaziridine **3** a fused silica column coated with Chirasil-β-Dex[55–57] (25 m × 0.25 mm i.d., 0.5 μm film thickness) was used. The dynamic measurements were repeated three times at each temperature in steps of 10 K between 100 and 160°C.

Evaluation by the Unified Equation

For the evaluation of the forward reaction rate constants k_1 with the unified equation[45–47] (1a and 1b), the total retention times of the enantiomers t_R^A and t_R^B, the hold-up time t_0, the plateau height h_p, the peak widths at half height w_h, the number of theoretical plates N, and the initial ratio $[A_0/B_0]$ are used.

If the signal intensity at the retention time t_R^A is higher or equal compared to the signal intensity at the retention time t_R^B eq. 1a has to be used.

$$k_1 = -\frac{1}{t_R^A}\left(\ln\left(\frac{100B_0+A_0\left(100-h_p\left(1+\sqrt{\frac{2}{\pi N}}\right)\right)}{t_R^B-t_R^A}\right) - \ln\left(B_0\left(\frac{h_p e^{-\frac{(t_R^A-t_R^B)^2}{2\sigma_B^2}} - 100e^{-\frac{(t_R^A-t_R^B)^2}{8\sigma_B^2}}}{\sigma_B\sqrt{2\pi}} + \frac{100}{t_R^B-t_R^A}\right) - A_0\left(\frac{100e^{-\frac{(t_R^B-t_R^A)^2}{8\sigma_A^2}} - h_p}{\sigma_A\sqrt{2\pi}} + \frac{h_p\left(1+\sqrt{\frac{2}{\pi N}}\right)-100}{t_R^B-t_R^A}\right)\right)\right) \quad (1a)$$

with $\sigma_i = \frac{w_i}{\sqrt{8\ln 2}}$ and $i = \{A, B\}$

If the peak at t_R^B is higher than at t_R^A eq. 1b has to be applied.

$$k_1 = -\frac{1}{t_R^A}\left(\ln\left(\frac{100A_0+B_0\left(100-h_p\left(1-\sqrt{\frac{2}{\pi N}}\right)\right)}{t_R^B-t_R^A}\right) - \ln\left(A_0\left(\frac{h_p e^{-\frac{(t_R^B-t_R^A)^2}{2\sigma_A^2}} - 100e^{-\frac{(t_R^B-t_R^A)^2}{8\sigma_A^2}}}{\sigma_A\sqrt{2\pi}} + \frac{100}{t_R^B-t_R^A}\right) - B_0\left(\frac{100e^{-\frac{(t_R^A-t_R^B)^2}{8\sigma_B^2}} - h_p}{\sigma_B\sqrt{2\pi}} + \frac{h_p\left(1-\sqrt{\frac{2}{\pi N}}\right)-100}{t_R^B-t_R^A}\right)\right)\right) \quad (1b)$$

The principle of microscopic reversibility[58] has been fully considered in eqs. 1a and 1b. Moreover, these

equations are no longer restricted to the evaluation of elution profiles of racemic mixtures. Calculations were performed with the software program DCXplorer (The software DCXplorer is available from the corresponding author as executable program running under Windows 2000, XP, and Vista).[59] Therefore, single elution profiles are directly integrated and evaluated in a graphical interface by zooming into the area of the interconversion profile.

Evaluation of Activation Parameters $\Delta H^{\ddagger}$ and $\Delta S^{\ddagger}$

For the evaluation experiments between 100 and 140°C were considered. At higher temperatures peak coalescence occurred and therefore rate constants could not be determined with sufficient precision. The Gibbs free activation energy $\Delta G^{\ddagger}(T)$ was calculated according to the Eyring eq. 2 where k_B is the Boltzmann constant ($k_B = 1.380662 \times 10^{-23}$ J K^{-1}), T is the enantiomerization temperature [K], h is Planck's constant ($h = 6.62617 \times 10^{-34}$ J s), and R is the gas constant ($R = 8.31441$ J K^{-1} mol^{-1}). The statistical factor κ was set to 0.5 for a reversible degenerated interconversion process.

$$\Delta G^{+}(T) = -RT \ln\left(\frac{k_1 h}{\kappa k_B T}\right) \quad (2)$$

As the studies were performed at temperatures between 100 and 140°C, the activation enthalpy $\Delta H^{\ddagger}$ of the enantiomerization was obtained from the slope and the activation entropy $\Delta S^{\ddagger}$ from the intercept of the Eyring plot ($\ln(k_1/T)$ vs. T^{-1}). Deviations of the activation parameters $\Delta H^{\ddagger}$ and $\Delta S^{\ddagger}$ have been calculated by error band analysis of the linear regression with a level of confidence of 95%.

RESULTS AND DISCUSSION

1,2-Di-*n*-propyldiaziridine **1** and 1,2-diisopropyldiaziridine **3** were synthesized from the corresponding amines by formation of the aminal with formaldehyde and oxidative ring closure with sodium hypochlorite (cf. Scheme 3) and isolated by vacuum distillation. 1-Isopropyl-2-*n*-propyldiaziridine **2** was obtained by statistical synthesis using *n*-propylamine and isopropylamine and was isolated from the other constitutional isomers by vacuum spinning band column distillation. The obtained diaziridines were completely characterized by ^{1}H and ^{13}C NMR spectroscopy (DEPT-135 and ^{1}H-^{13}C correlation NMR; cf. Fig. 1), as well as EI MS employing a quadrupole ion trap mass analyzer.

The enantiomer separation of 1,2-di-*n*-propyldiaziridine **1**, 1-isopropyl-2-*n*-propyldiaziridine **2**, and 1,2-diisopropyldiaziridine **3** was achieved by enantioselective gas chromatography using the chiral stationary phase (CSP) Chirasil-β-Dex.[55–57] The separation factors α are strongly influenced by the presence of the more bulky and rigid isopropyl group. While the separation factor α is only 1.04 for 1,2-di-*n*-propyldiaziridine **1**, α increases to 1.18 for 1-isopropyl-2-*n*-propyldiaziridine **2**, and 1.20 for 1,2-diisopropyldiaziridine **3** at 100°C.

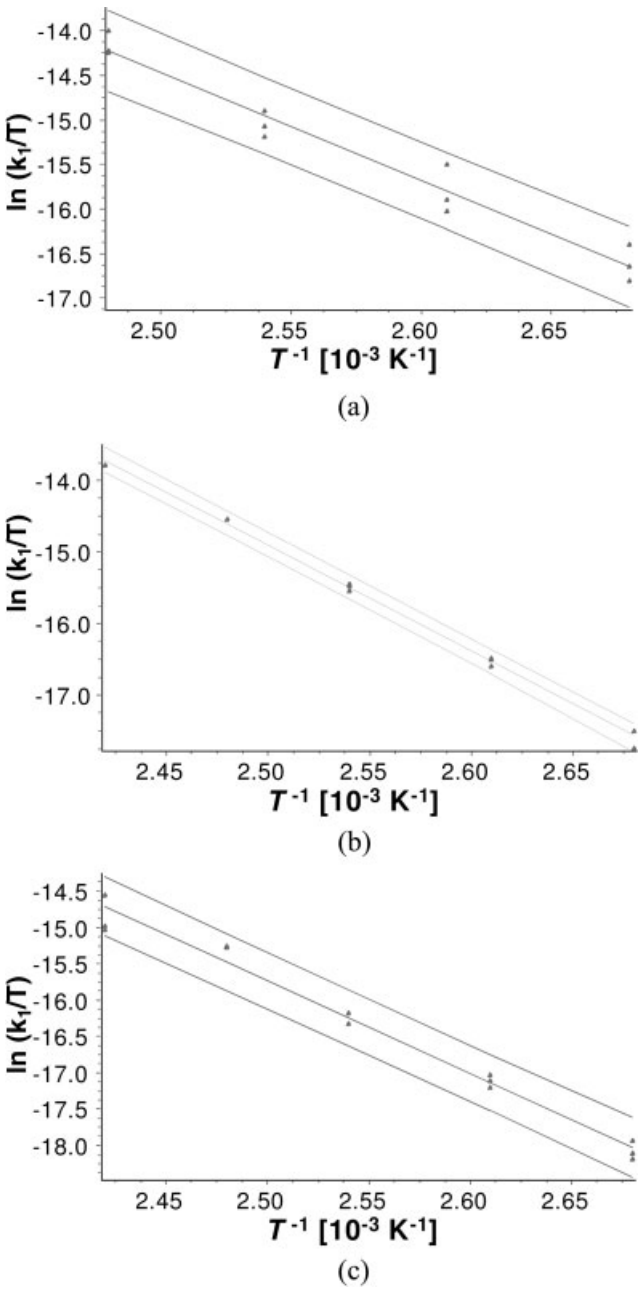

Fig. 3. Eyring plots for the determination of the activation parameters $\Delta H^{\ddagger}$ and $\Delta S^{\ddagger}$ of the enantiomerization of (**a**) 1,2-di-*n*-propyldiazirine, (**b**) 1-isopropyl-2-*n*-propyldiaziridine, and (**c**) 1,2-diisopropyldiaziridine from the enantioselective DGC experiments. The upper and lower curves represent the error bands of the linear regression with a level of confidence of 95%. For the linear regression, three measurements for each temperature were considered.

To determine the activation barrier $\Delta G^{\ddagger}$ and the activation parameters $\Delta H^{\ddagger}$ and $\Delta S^{\ddagger}$ of the enantiomerization of these propyl-substituted diaziridines (cf. Scheme 1), temperature-dependent enantioselective dynamic gas chromatography (DGC) was performed between 100 and 160°C. At 140°C coalescence occurred for 1,2-di-*n*-propyldiaziridine **1**, at 150°C for 1-isopropyl-2-*n*-propyldiaziridine **2**, and at 160°C for 1,2-diisopropyldiaziridine **3**. Elution

TABLE 2. Separation factors α (at 100°C/50 kPa He) and the activation parameters of the investigated 1,2-propyldiaziridines

Diaziridine	$\alpha_{100°C}$	$\Delta G^{\ddagger}_{100°C}$ (kJ mol^{-1})	$\Delta G^{\ddagger}_{298K}$ (kJ mol^{-1})	$\Delta H^{\ddagger}$ (kJ mol^{-1})	$\Delta S^{\ddagger}$ (J K^{-1} mol^{-1})	r	s_y
 **1**	1.04	125.3 ± 0.6	118.7	100.7 ± 2.1	−60 ± 3	0.9978	0.0663
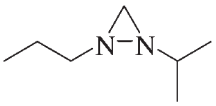 **2**	1.18	128.3 ± 0.4	123.3	113.7 ± 2.5	−33 ± 1	0.9933	0.1297
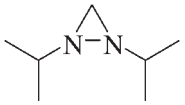 **3**	1.24	129.8 ± 0.4	123.3	106.5 ± 2.0	−56 ± 2	0.9951	0.1210

r denotes the correlation coefficient and s_y is the residual deviation of the linear regression of the Eyring plots.

profiles of the diaziridines between 100°C and 150°C are depicted in Figure 2.

Reaction rate constants k of enantiomerization were calculated with the analytical function of the unified equation[45–47] (eqs. 1a and 1b) considering three experiments at each temperature. Elution profiles showing coalescence at elevated temperature were not considered for the calculation of the reaction rate constants. Experimental data of 1,2-diisopropyldiaziridine **3** determined from the elution profiles and the calculated reaction rate constants are summarized in Table 1.

The activation enthalpies $\Delta H^{\ddagger}$ and activation entropies $\Delta S^{\ddagger}$ of the three diaziridines were obtained by plotting $\ln(k_1/T)$ as a function of T^{-1} according to the Eyring equation (cf. Fig. 3).

By linear regression analysis, the activation parameters could be determined and are summarized in Table 2.

These enantiomerization barriers are in very good agreement with previously determined values for 1,2-di-*tert*-butyldiaziridine ($\Delta H^{\ddagger}$ = 113.0 ± 2.0 kJ mol^{-1} and $\Delta S^{\ddagger}$ = 44 ± 5 J K^{-1} mol^{-1}), 1,2-di-*n*-butyldiaziridine ($\Delta H^{\ddagger}$ = 118.9 ± 1.0 kJ mol^{-1} and $\Delta S^{\ddagger}$ = 17 ± 3 J K^{-1} mol^{-1}), and 1-*n*-butyl-2-*tert*-butyldiaziridine ($\Delta H^{\ddagger}$ = 112.6 ± 2.5 kJ mol^{-1} and $\Delta S^{\ddagger}$ = 27 ± 2 J K^{-1} mol^{-1}). A comparison of the enantiomerization barriers of the diaziridines investigated here reveals a significant increase for the more sterically demanding isopropyl group. However, the second isopropyl group in 1,2-diisopropyldiaziridine **3** does not significantly contribute as it is expected for two sterically demanding groups to increase even more the barrier by steric hindrance. Furthermore, the enantiomerization barrier of 1-isopropyl-2-*n*-propyldiaziridine **2** and 1,2-diisopropyldiaziridine **3** are similar. There is also a significant difference in the activation enthalpy $\Delta H^{\ddagger}$ and entropy $\Delta S^{\ddagger}$ of 1-isopropyl-2-*n*-propyldiaziridine **2** compared to diaziridines **1** and **3**. The increase of the activation entropy $\Delta S^{\ddagger}$ can be attributed to the increased number of possible states, because of the unsymmetrical substitution pattern.

Taking into consideration that the enantiomerization barrier of 1-isopropyl-2-*n*-propyldiaziridine **2** is different from the mean enantiomerization barrier of diaziridines **1** and **3** and that the activation entropies $\Delta S^{\ddagger}$ are negative, an interconversion mechanism via electrocyclic ring opening ring closure mechanism with charge separation in the transition state can be suggested (cf. Scheme 1).

In conclusion, this investigation of the diaziridines 1,2-di-*n*-propyldiaziridine **1**, 1-isopropyl-2-*n*-propyldiaziridine **2**, and 1,2-diisopropyldiaziridine **3** demonstrates that enantioselective gas chromatography (DGC) and direct evaluation of the obtained elution profiles by the unified equation constitutes a valuable and straightforward tool for the measurement of enantiomerization barriers to look into mechanistic aspects of the interconversion process. The study of structurally related sets of compounds under the same experimental conditions gives further insights into the stereodynamics. We have shown that the enantiomerization barrier of diaziridines does not necessarily correlate with increasing steric hindrance by sterically demanding substituents. Furthermore, the results suggest that the interconversion in diaziridines proceeds via an electrocyclic ring opening ring closure mechanism.

LITERATURE CITED

1. Wüthrich K. NMR-untersuchungen von struktur und funktion biologischer makromoleküle (Nobel-Vortrag). Angew Chem 2003;115: 3462–3486.
2. Heegaard NHH, Jorgensen TJD, Cheng L, Schou C, Nissen MH, Trapp O. Interconverting conformations of variants of the human amyloidogenic protein ß2-microglobulin quantitatively characterized by dynamic capillary electrophoresis and computer simulation. Anal Chem 2006;78:3667–3673.
3. Reist M, Testa B, Carrupt PA. The racemization of enantiopure drugs: helping medicinal chemists to approach the problem. Enantiomer 1997;2:147–155.
4. Werner A. Über die räumliche anordnung der atome in stickstoffhaltigen molekülen, Doctoral Thesis. Zürich. Polytechnikum Zürich: Polytechnikum Zürich; 1890.
5. Lambert JB. Pyramidal atomic inversion. Top Stereochem 1971;6:19–105.
6. Prelog V, Wieland P. Über die spaltung der Tröger'schen base in optische antipoden, ein beitrag zur stereochemie des dreiwertigen stickstoffs. Helv Chim Acta 1944;27:1127–1134.
7. Tröger J. Über einige mittels nascierenden formaldehyds entstehende Basen. J Prakt Chem 1887;36:225–245.
8. Mannschreck A, Radeglia R, Gründemann E, Ohme R. Der diaziridinring als asymmetriezentrum. Chem Ber 1967;100:1778–1785.
9. Mannschreck A, Seitz W. Trennung inversionsisomerer diaziridine. langsame inversion am dreibindigen stickstoffatom. Angew Chem 1969;81:224.
10. Häkli H, Mintas M, Mannschreck A. Preperative separations of enantiomeric diaziridines by liquid chromatography on triacetylcellulose. Racemizations monitored by polarimetry and by 1H-NMR. Chem Ber 1979;112:2028–2038.
11. Brois SJ. Aziridines. XII. Isolation of a stable nitrogen pyramid. J Am Chem Soc 1968;90:508–509.
12. Felix D, Eschenmoser A. Langsame inversion am pyramidal gebundenen stickstoff: isolierung von diastereomeren 7-Chlor-7-azabicyclo[4.0.1]heptanen bei raumtemperatur. Angew Chem 1968;80:197–199.
13. Lehn JM, Wagner J. Hindred nitrogen inversion in n-halogenaziridines and in n-halogenazetidines. Chem Commun 1968;148–150.
14. Kostyanovsky RG, Tchervin II, Fomichov AA, Samojlova ZE, Makarov CN, Zeifman YuV, Dyatkin BL. Nitrogen inversion in n-substituted 2,2-bis(trifluoromethyl)aziridines. Tetrahedron Lett 1969;46:4021–4024.
15. Brois SJ. Stable nitrogen pyramids. IV. 1-Alkoxyaziridines. a new aziridine synthesis via O-nitrenes. J Am Chem Soc 1970;92:1079–1080.
16. Shustov GV, Kadorkina GK, Kostyanovsky RG, Rauk A. Asymmetric nitrogen. 67. Geminal systems. 41. Chiroptical properties of n-chloro and n-bromo derivatives of three-membered nitrogen heterocycles: aziridines and diaziridines. J Am Chem Soc 1988;110:1719–1726.
17. Lambert JB, Takeuchi Y. Cyclic organonitrogen stereodynamics. New York. VCH: VCH; 1992.
18. Schurig V, Bürkle W, Zlatkis A, Poole CF. Quantitative resolution of pyramidal nitrogen invertomers by complexation chromatography. Naturwissenschaften 1979;66:423–424.
19. Rudchenko VF, D'Yachenko OA, Zolotoi AB, Atovmyan LO, Chervin II, Kostyanovsky RG. Asymmetrical nonbridgehead nitrogen—xxiv: complete separation into antipodes and absolute configuration of chiralic n-alkoxyaziridines. Tetrahedron 1982;38:961–975.
20. Andersonza JE, Lehn JM. Nuclear magnetic resonance studies of rate processes and conformations. V. synchronous inversion at two nitrogens. J Am Chem Soc 1967;89:81–87.
21. Lehn JM. Nitrogen inversion—experiment and theory. Top Curr Chem 1970;15:311–377.
22. Kostyanovsky RG, Kadorkina GK, Kostyanovsky VR, Schurig V, Trapp O. Außerordentliche sterische hinderung der stickstoffinversion in 1,3,4-oxadiazolidinen. Angew Chem 2000;112:3066–3069.
23. Kostyanovsky RG, Kadorkina GK, Kostyanovsky VR, Schurig V, Trapp O. Pronounced steric hindrance for nitrogen inversion in 1,3,4-oxadiazolidines. Angew Chem Int Ed Engl 2000;39:2938–2940.
24. Huisgen R, Scheer W, Huber H. Stereospecific conversion of cis-trans isomeric aziridines to open chain azomethine ylides. J Am Chem Soc 1967;89:1753–1755.
25. Huisgen R. Elektrocyclische ringöffnungen von ethylenoxiden. Angew Chem 1977;89:689–602.
26. Huisgen R. Electrocyclic ringopenings of epoxides. Angew Chem Int Ed Engl 1977;16:572–585.
27. Trapp O, Schurig V, Kostyanovsky RG. The control of the nitrogen inversion in alkylsubstituted diaziridines. Chem Eur J 2004;10:951–957.
28. Binsch G, Kessler H. Die kinetische und mechanistische Auswertung von NMR-spektren. Angew Chem 1980;92:445–463.
29. Binsch G, Kessler H. The Kinetic and mechanistic evaluation of NMR spectra. Angew Chem Int Ed Engl 1980;19:411–494.
30. Weseloh G, Wolf C, König WA. A new application of capillary zone electrophoresis: determination of energy barriers of configurationally labile chiral compounds. Angew Chem Int Ed Engl 1995;34:1635–1636.
31. Weseloh G, Wolf C, König WA. Eine neue Anwendung de Kapillarzonenelektrophorese: Best immuny der Energic barriere von Konfigurationslabilen Verbindungen. Angew Chem 1995;107:1771–1772.
32. Reich S, Trapp O, Schurig V. Enantioselective stopped-flow multidimensional gas chromatography—determination of the inversion barrier of 1-chloro-2,2-dimethylaziridine. J Chromatogr A 2000;892:487–498.
33. Trapp O, Schurig V. Stereointegrity of Tröger's base: gas-chromatographic determination of the enantiomerization barrier. J Am Chem Soc 2000;122:1424–1430.
34. Schurig V, Bürkle W, Zlatkis A, Poole CF. Quantitative resolution of pyramidal nitrogen invertomers by complexation chromatography. Naturwissenschaften 1979;66:423–424.
35. Trapp O, Schoetz G, Schurig V. Determination of enantiomerization barriers by dynamic and stopped flow chromatographic methods. Chirality 2001;13:403–414.
36. Wolf C. Stereolabile chiral compounds: analysis by dynamic chromatography and stopped-flow methods. Chem Soc Rev 2005;595–608.
37. Krupcik J, Oswald P, Majek P, Sandra P, Armstrong DW. Determination of the interconversion energy barrier of enantiomers by separation methods. J Chromatogr A 2003;1000:779–800.
38. D'Acquarica I, Gasparrini F, Pierini M, Villani C, Zappia G. Dynamic HPLC on chiral stationary phases: a powerful tool for the investigation of stereomutation processes. J Sep Sci 2006;29:1508–1516.
39. Schurig V. Peak coalescence phenomena in enantioselective chromatography. Chirality 1998;10:140–146.
40. Jung M, Schurig V. Determination of enantiomerization barriers by computer simulation of interconversion profiles: enantiomerization of diaziridines during chiral inclusion gas chromatography. J Am Chem Soc 1992;114:529–534.
41. Keller RA, Giddings JC. Multiple zones and spots in chromatography. J Chromatogr 1960;3:205–220.
42. Dondi F, Cavazzini A, Remelli M. The stochastic theory of chromatography. Adv Chromatogr 1998;38:51–70.
43. Trapp O, Schurig V. Approximation function for the direct calculation of rate constants and Gibbs activation energies of enantiomerization of racemic mixtures from chromatographic parameters in dynamic chromatography. J Chromatogr A 2001;911:167–175.
44. Trapp O, Schurig V. Novel direct access to enantiomerization barriers from peak profiles in enantioselective dynamic chromatography: enantiomerization of dialkyl-1,3-allenedicarboxylates. Chirality 2002;14: 465–470.
45. Trapp O. Unified equation for access to rate constants of first-order reactions in dynamic and on-column reaction chromatography. Anal Chem 2006;78:189–198.
46. Trapp O. The unified equation for the evaluation of first order reactions in dynamic electrophoresis. Electrophoresis 2006;27:534–541.

47. Trapp O. Fast and precise access to enantiomerization rate constants in dynamic chromatography. Chirality 2006;18:489–497.
48. Trapp O, Weber SK, Bauch S, Hofstadt W. Hochdurchsatz-Screening von Katalysatoren durch Integration von Reaktion und Analyse. Angew Chem 2007;119:7447–7451.
49. Trapp O, Weber SK, Bauch S, Hofstadt W. High-throughput screening of catalysts by combining reaction and analysis. Angew Chem Int Ed Engl 2007;46:7307–7310.
50. Trapp O, Weber SK, Bauch S, Bäcker T, Hofstadt W, Spliethoff B. High throughput kinetic study of hydrogenations over palladium nanoparticles—combination of reaction and analysis. Chem Eur J 2008;14:4657–4666.
51. Trapp O. High-throughput monitoring of interconverting stereoisomers and catalytic reactions. Chem Today 2008;26:26–28.
52. Trapp O. A dynamic molecular probe to investigate catalytic effects and joule heating in enantioselective micellar electrokinetic chromatography. Electrophoresis 2007;28:691–696.
53. Trapp O. Gas chromatographic high-throughput screening techniques in catalysis. J Chromatogr A 2008;1184:160–190.
54. Ohme R, Schmitz E, Dolge P. Diaziridine aus Aminalen des Formaldehyde. Chem Ber 1966;99:2104–2109.
55. Schurig V, Schmalzing D, Schleimer M. Enantiomerentrennungen an immobilisiertem Chirasil-Metall und Chirasil-Dex durch Gaschromatographie mit überkritischen Gasen. Angew Chem 1991;103:994–996.
56. Schurig V, Schmalzing D, Schleimer M. Enantiomer separation on immobilized chirasil-metal and chirasil-dex by gas chromatography and supercritical fluid chromatography. Angew Chem Int Ed Engl 1991; 30:987–989.
57. Cousin H, Trapp O, Peulon-Agasse V, Pannecoucke X, Banspach L, Trapp G, Jiang Z, Combret JC, Schurig V. Synthesis, NMR characterisation and polysiloxane-based immobilization of the three regioisomeric monooctenylpermethyl-β-cyclodextrins—application in enantioselective GC. Eur J Org Chem 2003;3273–3287.
58. Bürkle W, Karfunkel H, Schurig V. Dynamic phenomena during enantiomer resolution by complexation gas chromatography. J Chromatogr 1984;288:1–14.
59. Trapp O. A novel software tool for high throughput measurements of interconversion barriers: DCXplorer. J Chromatogr B 2008;875:42–47.